The Electronic Spectra of Pyrene, Chrysene, Azulene, Coronene and Tetracene Crystals

By Jiro TANAKA

(Received July 14, 1964)

The theory of molecular exciton developed by Davydov and others has been widely used for the interpretation of the crystal spectrum, and a lot of results have been published which confirm a validity of the theory in general.[1] However, when a molecule has many excited levels, a mixing of excited states may occur between weak, medium and strong intensity bands and a spectrum may became so complicated that a simple correlation cannot be made between molecular and crystalline absorption bands.

In the present paper the electronic absorption spectra of single crystals of pyrene, chrysene, azulene, coronene and tetracene are reported in an attempt to affirm the theory; a particular effort will be made to find the mechanism of the intermolecular electronic interaction of the excited states in crystals.

The hydrocarbons cited above are characterized by having many strong absorptions in the near ultraviolet and relatively lower ionization potentials. The dipolar interaction between the excited levels might be very strong in such crystals, and the charge transferred level will be located at a relatively low energy region. The band splittings and intensities are calculated by including the configuration interaction between several excited states, and the results are compared with observed absorption bands.

Although the general features of the spectra can be explained very well, a discrepancy is noticed with some crystals, particularly in the intensities of very strong and very weak bands. The strong band is weakened and the weak band is strengthened more than would be expected from the dipole-dipole interaction scheme. The hypochromism of the stronger band may arise from the interaction with the ionization continuum level, and the hyperchromism of the weaker band may occur as a result of the higher order interaction with allowed transitions. Also the calculated splitting of some crystals does not agree completely

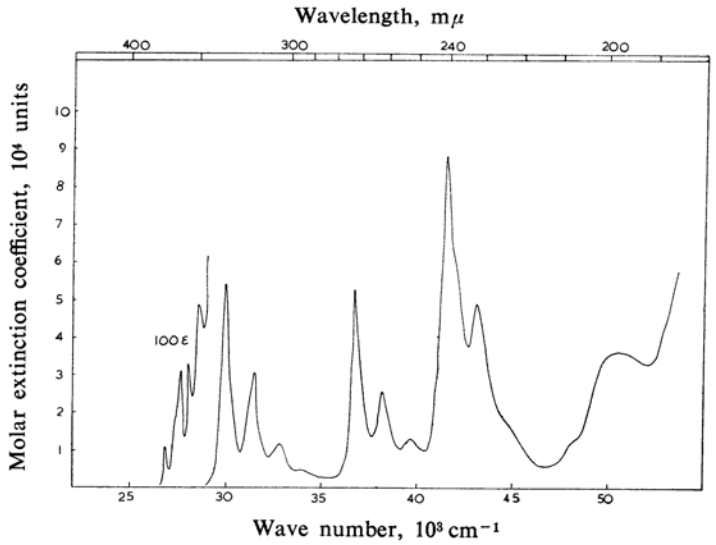

Fig. 1. Absorption spectrum of pyrene in *n*-heptane.

1) D. S. McClure, *Solid State Physics*, **8**, 1 (1958); J. Tanaka, *Prog. Theoret. Phys., Suppl.*, **12**, 183 (1959); A. S. Davydov, "Theory of Molecular Exciton" (translated by M. Kasha and M. Oppenheimer, Jr.), McGraw-Hill, New York (1962); D. P. Draig and S. H. Walmsley, "Physics and Chemistry of the Organic Solid State," Vol. I, Ed. by Fox, Labes and Weissberger, Interscience Publishers, New York (1963), p. 586.

with the experimental results; this may suggest a need for more elaborate calculations, including that of the electron overlap effect.

Experimental

The ultraviolet and visible spectra of *n*-heptane solutions were measured by a Cary recording spectrophotometer, model 14. The crystal spectra were measured by an ultraviolet microspectrophotometer described in a previous paper.[2] All the samples were purified by recrystallization or chromatography, followed by sublimation. The thin crystals suitable for spectral measurement were prepared by sublimation. The thicknesses of these crystals were roughly estimated by means of the interference color as seen under a polarization microscope.

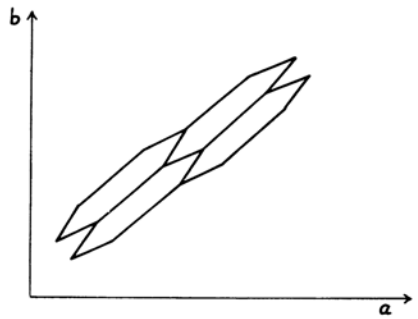

Fig. 2 (a). Projection of pyrene molecule onto the (001) plane.

Pyrene

Five absorption bands have been observed in a *n*-heptane solution, as Fig. 1 and Table I show. Ham and Rudenberg[3] predicted that transitions to the ^1L_b and ^1B_a states are possible along the short-axis (M-axis) of the molecule, while the ^1L_a and ^1B_b transitions are active along the long-axis (L-axis). The crystalline spectrum (Fig. 2 (b)) has been recorded using a crystal about 0.4 μ thick* through the (001) plane and with a light polarized along the a- and b-axes. The projection of the molecules onto the (001) plane, based on the X-ray crystal analysis results of Robertson and White,[4] is shown in Fig. 2 (a). The wave functions of the crystalline exciton state are given by the following formula for each excited state:

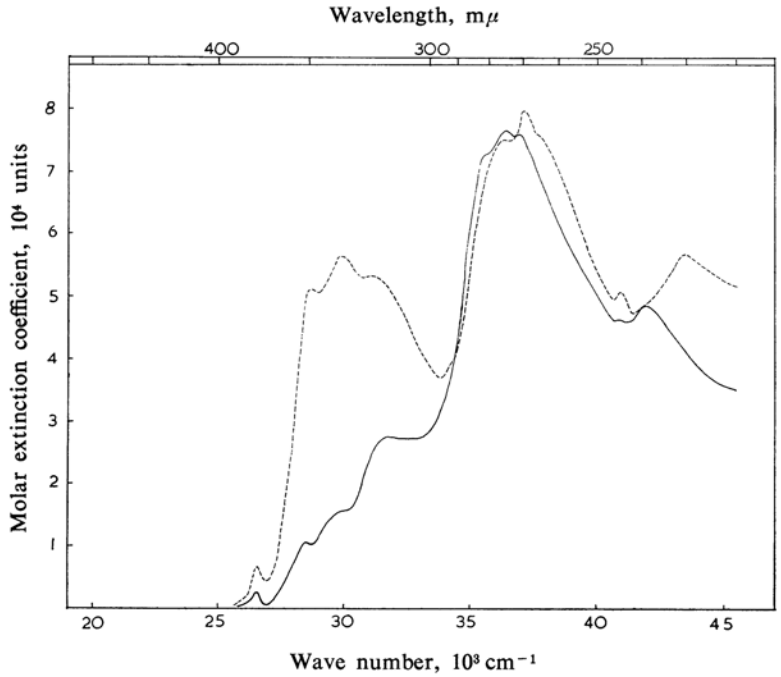

Fig. 2 (b). Polarized absorption spectrum of pyrene crystal.
—— The light polarized parallel to the b-axis
---- The light polarized parallel to the a-axis

2) J. Tanaka, This Bulletin, **36**, 833 (1963).

* The thickness of the crystal is estimated by means of the retardation color, assuming that the birefringence between the a- and b-axes is 0.125.

3) N. S. Ham and K. Rudenberg, *J. Chem. Phys.*, **25**, 14 (1956).

4) J. M. Robertson and J. G. White, *J. Chem. Soc.*, **1947**, 358.

TABLE I. ABSORPTION BANDS OF PYRENE

	Solution			Crystal (Observed)				Crystal (Calculated)			
	cm^{-1}	f	μ, Å	a-axis	b-axis	splitting	$f_a : f_b$ (d. r.)*	a-axis	b-axis	splitting	$f_a : f_b$ (d. r.)
^1L_b	26880 27400 28050 28580	0.0016	0.074	26600	26600	0	0.0019 : 0.0011 (1.7 : 1.0)	26884	26883	1	0.0015 : 0.0011 (1.35 : 1.0)
^1L_a	29920 31500 32850 34000	0.15 0.12 0.06	0.68 0.59 0.39	28570 29760 (31056)** (31447)	28328 29630 (31250) (31847) (32787)	242 130 −200	0.12 : 0.03 (4.2 : 1.0)	30158 31728 32968	29909 31485 32840	249 243 128	0.193 : 0.026 (7.4 : 1.0)
^1B_a	36710 38170 39700	0.35	0.935	35700 37070 37624	35138 36600 37067	562 470 563	0.20 : 0.19 (1.05 : 1.0)	37395	37285	100	0.412 : 0.315 (1.3 : 1.0)
^1B_b	41480 43100 50500	0.85	1.36	42000	39500 40300	1700	0.15 : 0.12 (1.2 : 1.0)	42826	41795	1020	0.58 : 0.43 (1.35 : 1.0)

* d. r. is an abbreviation for the dichroic ratio.
** Those bands are regarded as the charge-transfer transitions.

$$\left.\begin{aligned}\Psi^{\alpha} &= \frac{1}{\sqrt{4N}}\Big(\sum_{i=1}^{N}\phi_{1i}' - \sum_{j=1}^{N}\phi_{2j}' \\ &\quad - \sum_{k=1}^{N}\phi_{3k}' + \sum_{l=1}^{N}\phi_{4l}'\Big); \quad B_u \\ \Psi^{\beta} &= \frac{1}{\sqrt{4N}}\Big(\sum_{i=1}^{N}\phi_{1i}' - \sum_{j=1}^{N}\phi_{2j}' \\ &\quad + \sum_{k=1}^{N}\phi_{3k}' - \sum_{l=1}^{N}\phi_{4l}'\Big); \quad A_u\end{aligned}\right\} \quad (1)$$

where ϕ_{1i}' denotes the excited state in which the 1st site molecule in the i-th cell is excited while the others are in the ground state. The coordinate of the molecule on each site is chosen following the notation of the International Table,[5] namely, 1 (x, y, z), 2 $(\bar{x}, \bar{y}, \bar{z})$, 3 $(1/2-x, 1/2+y, \bar{z})$ and 4 $(1/2+x, 1/2-y, z)$. The first-order energy levels are given by Eq. 2 for each excited state:

$$\left.\begin{aligned}&E^{\alpha} = E_0 + V_{11} - 1/2V_{12} - 1/2V_{13} + 1/2V_{14} \\ &E^{\beta} = E_0 + V_{11} - 1/2V_{12} + 1/2V_{13} - 1/2V_{14} \\ &V_{kl} = \\ &\sum_{i=1}^{N}\int \phi_k^{*\prime}(1)\phi_{li}^{*}(2)\, V\phi_k(1)\phi_{li}'(2)\mathrm{d}\tau_1\mathrm{d}\tau_2\end{aligned}\right\} \quad (2)$$

where E_0 indicates the energy of the molecular excited state, including a small shift due to interaction between the excited state and the ground state. V is the intermolecular potential, ϕ_k and ϕ_k' represent the ground- and the excited-state wave function of the k-th site molecule, and ϕ_l and ϕ_l' are those of l-th site molecule.

Actually, we have taken only the dipole-dipole interaction term, and the calculations have been carried out by the method of direct summation over molecules inside the restricted radius sphere. The ISSP Facom 202 computer has been used; the results are shown in Appendix I. It may be seen that the value obtained by the summation over a 30 Å radius sphere is very close to the value of a 50 Å radius sphere. Craig and Walmsley[1] published the results of similar calculations by the Ewald-Kornfeld's method; it is very interesting that the present results are in good agreement with their values in spite of the different computational procedures. The convergence of a direct summation seems to be sufficient if we take the summation within a 50 Å radius sphere.

Since we are considering four excited levels in the present case, it might be necessary to calculate the second order interaction between those levels. The secular equation is given by:

$$\left.\begin{aligned}&\mathrm{Det}\,|H_{rs} - E\delta_{rs}| = 0 \\ &H_{rs} = \int \Psi_r^{\alpha} H \Psi_s^{\alpha}\,\mathrm{d}\tau, \\ \text{or} \quad &H_{rs} = \int \Psi_r^{\beta} H \Psi_s^{\beta}\,\mathrm{d}\tau \\ &H = H_0 + V, \ \delta_{rs} = 1 \text{ when } r = s, \\ &\delta_{rs} = 0 \text{ when } r \neq s\end{aligned}\right\} \quad (3)$$

where H indicates the total Hamiltonian of the system, and Ψ_r and Ψ_s represent the r-th and s-th excited levels (^1L_b, ^1L_a, ^1B_a or ^1B_b states). The interaction between B_u and A_u-type functions vanishes for symmetry reasons. The diagonal element is taken as a first-order

5) "International Tables for X-ray Crystallography," Vol. I, Kynoch Press, Birmingham (1959).

exciton energy calculated by Eq. 2, while the off-diagonal term is calculated by a similar equation using the dipole approximation. For the ^1L_a band we have considered three vibrational levels separately; this implies a weak coupling between the ^1L_a state and other states. The secular equation is shown in Appendix II. Solving this equation, the wave function for the L-th crystal excited state is obtained as a linear combination of excited states Ψ_r:

$$\Psi_L{}^\alpha = \sum a_r \Psi_r{}^\alpha, \qquad \Psi_L{}^\beta = \sum b_r \Psi_r{}^\beta \tag{4}$$

and the transition moment, say, to the α state is given by a sum of the composite transition moments projected along the particular crystalline axis:

$$M_{OL}{}^\alpha = \int \Psi_0{}^* \boldsymbol{r} (\sum a_r \Psi_r{}^\alpha) \mathrm{d}r = \sum a_r M_{or} \cos\theta_{ar} \tag{5}$$

where M_{or} is the magnitude of the transition moment to the r-th state, and θ_{ar} is the angle between the transition moment and the a-axis. The oscillator strength of the crystalline absorption band is calculated by Eq. 6:

$$f_{OL} = 3.25 \times 10^{-5} \times \nu \times (M_{OL}{}^\alpha)^2 \tag{6}$$

The second-order perturbation effect for the ground state (van der Waals force) has been disregarded. The results of the calculation are given in Table I and Fig. 3.

At room temperature the observation of the band splitting is not very feasible, but it may be clearly seen in Fig. 2(b) that both the ^1L_a and ^1B_a bands show appreciable splittings. By comparing the calculated intensity ratio with the observed spectrum, it is easy to prove the theoretical results of Ham and Rudenberg concerning the polarization of the bands. The first ^1L_b band, the weakest of all, might be influenced by the nearby stronger transition, and it shows the dichroic ratio $D_a : D_b = 1.7 : 1.0$, while the second-order calculation value is 1.35 : 1.0. The oriented gas value (the zeroth and first-order approximation) of 1.0 : 1.0 is improved by the second-order calculation, and it is almost certain that the ^1L_b state is short-axis polarized. The conclusion is in agreement with the earlier findings of Ferguson.[6]

Pyrene

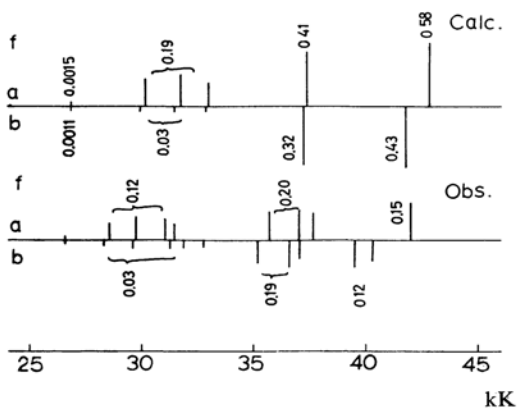

Fig. 3. Calculated and observed band positions of pyrene crystal.

The ^1L_a band shows four or more vibrational structures in the crystalline spectrum, the first and the second peaks being split about 240 cm^{-1} and 130 cm^{-1}. The calculated values, 249 cm^{-1} and 243 cm^{-1} respectively, are in excellent agreement with the observed values. The splittings of the third and fourth peaks are reversed in sign; therefore, it might be possible that those peaks have a different origin. The charge-transfer transition might be very probable in such a crystal as pyrene, where molecules are placed in pairs, and it has been observed in the case of perylene.[7] The fluorescence of pyrene crystal has been established to originate from an excited dimeric state,[6] and the corresponding absorption should exist at a higher energy region. Following the recent theory of Murrell and Tanaka[8] on the spectra of the pyrene dimer, it is expected that the intermolecular charge-transfer band will appear in the 30000 cm^{-1} spectral region when molecular planes are separated by about 3.5 Å. Therefore, the band near the 31000 cm^{-1} region is regarded as charge-transfer band overlapped with the progression of the ^1L_a band. The polarization of the ^1L_a band is deduced from the dichroic intensity ratio to be long-axis, because the observed value of 4.2 : 1.0 is close to the calculated value of 7.4 : 1.0 (that of the zeroth and first-order value is 5 : 1), while the short-axis assignment will give a value of about 1.0 : 1.0.

The band system at about 35000 cm^{-1} is clearly demonstrated by the intensity relations to be the short-axis polarized band. It shows splittings of 562, 470 and 563 cm^{-1} for each vibrational progression; these values should be compared with the calculated value of 110 cm^{-1} (strong coupling model). The first-order splitting was -37 cm^{-1}; therefore, the second-order calculation gives the right sign and the correct order of magnitude. The calculated intensity ratio, $D_a : D_b = 1.31 : 1.0$, is in good agreement with the observed value. The ^1B_b band is predicted to be at about 40000 cm^{-1}, but we see rather weaker absorptions in this region. Presumably the ^1B_b band is merged with the transitions to the ionization continuum state, and the original intensity is shared with the

6) J. Ferguson, *J. Chem. Phys.*, **28**, 765 (1958).
7) J. Tanaka, This Bulletin, **36**, 1237 (1963).
8) J. N. Murrell and J. Tanaka, *Mol. Phys.*, **7**, 363 (1964).

band at higher frequencies. The mechanism of this sort of interaction requires further investigation.

The thickness of the crystal could not be determined accurately enough to discuss the accurate value of the intensity of the crystal absorption; however, it seems certain that a hypochromism occurs in the ^1L_a, ^1B_a and ^1B_b bands. Contrary to this the ^1L_b band intensity is nearly in agreement with the value of the second-order theory. Therefore, the deviations of the absorption intensities of the stronger band should be ascribed to a mechanism which has not been considered in the above treatment.

Chrysene

Five absorption bands have been found in a *n*-heptane solution (Fig. 4); the band positions are tabulated in Table II, together with the theoretical assignment of Ham and Rudenberg.[3] The crystal structure analysis of chrysene was made by Iball;[9] the projection of molecules onto the (001) plane is pictured Fig. 5(a). The crystalline spectrum has been measured through the (001) plane by a polarized light (Fig. 4(b)). The thickness of the crystal has been estimated to be 0.25 μ by the use of optical data on the birefringence of Krc.[10] Since we are using a convergent light of a microscope lens, the absolute intensity of a band whose transition moment is vertical to the developed plane might not be accurate enough to discuss the direction of the transition moment on the basis of the dichroic intensity ratio. In the crystal spectrum the intensity is weaker with the light polarized along the a-axis than with that polarized along the b-axis for all absorption bands. Theoretical calculation[3] showed that the strongest ^1B_b band is polarized along the long-axis of the molecule and that the long-axis is nearly perpendicular to the b-axis; therefore, it seems to be unreasonable that the ^1B_b band is weaker along the a-axis than along the b-axis. This anomaly of intensity relation is clarified by the second-order calculations including interactions between ^1L_b, ^1L_a, ^1B_b and ^1B_a states. The crystal excited-state wave functions which are active along the a- and b-axes are:

$$\left.\begin{aligned}\Psi^{\alpha} &= \frac{1}{\sqrt{4N}}\left(\sum_{i=1}^{N}\psi_{1i}' + \sum_{j=1}^{N}\psi_{2j}' - \sum_{k=1}^{N}\psi_{3k}' - \sum_{l=1}^{N}\psi_{4l}'\right)\\ \Psi^{\beta} &= \frac{1}{\sqrt{4N}}\left(\sum_{i=1}^{N}\psi_{1i}' + \sum_{j=1}^{N}\psi_{2j}' + \sum_{k=1}^{N}\psi_{3k}' + \sum_{l=1}^{N}\psi_{4l}'\right)\end{aligned}\right\} \quad (7)$$

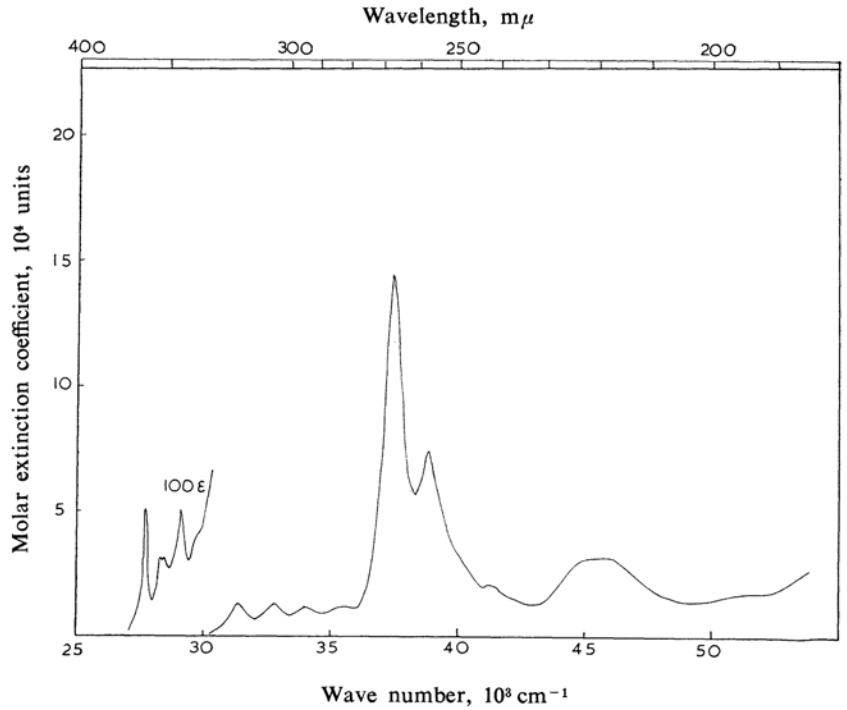

Fig. 4. Absorption spectrum of chrysene in *n*-heptane.

9) J. Iball, *Proc. Roy. Soc.*, **A146**, 140 (1934).

10) J. Krc, Jr., *Anal. Chem.*, **23**, 932 (1951).

TABLE II. ABSORPTION BANDS OF CHRYSENE

	Solution			Crystal (Observed)				Crystal (Calculated)			
	cm^{-1}	f	μ	a-axis	b-axis	splitting	$f_a : f_b$ (d. r.)	a-axis	b-axis	splitting	$f_a : f_b$ (d. r.)
	27730	0.00076	0.05	27470	27470	0	0.0017 : 0.005 (1.0 : 3.2)	27728	27728	0	0.00054 : 0.0013 (1.0 : 2.4)
^1L_b	28320			28120 28875	28120 28875						
	31350	0.08	0.49	30580	30090	490	0.042 : 0.092	31387	31170	217	0.136 : 0.382
^1L_a	32750	0.07	0.44	31555	31555	0	(1.0 : 2.2)	32739	32622	117	(1.0 : 2.8)
	34030	0.06	0.40	32880	32980	−100		33981	33929	52	
	35420	0.04	0.35		34210			35333	35467	−134	
^1B_b	37320	0.95	1.58	36780	36780	0	0.17 : 0.295 (1.0 : 1.7)	37517	37611 37839		0.246 : 0.825 (1.0 : 3.3)
	38860						0.06 : 0.08	45863			0.164
^1B_a	40000 41300	0.48	1.00	41400	40000						
	45000	0.60	1.10	44200?							

where ψ_{1i}', ψ_{2j}', ψ_{3k}' and ψ_{4l}' represent the excited state in which a molecule at the 1i-th, 2j-th, 3k-th or 4l-th site, respectively, is excited while the others are in their ground state. The coordinates of molecules are chosen following the space group notation of C_{2h}^6 I (2/C): $1(x, y, z)$, $2(1/2+x, 1/2+y, 1/2+z)$, $3(1/2-x, 1/2+y, z)$ and $4(\bar{x}, y, 1/2-z)$. The diagonal and the off-diagonal elements of the energy matrix are give for α and β states by:

$$\left.\begin{aligned}
&\int \Psi_m{}^{\alpha} H \Psi_m{}^{\alpha} d\tau = \\
&E_m + <m|V_{11} + 1/2 V_{12} - 1/2 V_{13} \\
&- 1/2\ V_{14}|m> \\
&\int \Psi_m{}^{\alpha} H \Psi_n{}^{\alpha} d\tau = \\
&<m|V_{11} + 1/2 V_{12} - 1/2 V_{13} \\
&- 1/2 V_{14}|n> \\
&\int \Psi_m{}^{\beta} H \Psi_m{}^{\beta} d\tau = \\
&E_m + <m|V_{11} + 1/2 V_{12} + 1/2 V_{13} \\
&+ 1/2\ V_{14}|m> \\
&\int \Psi_m{}^{\beta} H \Psi_n{}^{\beta} d\tau = \\
&<m|\ V_{11} + 1/2 V_{12} + 1/2 V_{13} \\
&+ 1/2 V_{14}|n>
\end{aligned}\right\} \quad (8)$$

where $\Psi_m{}^{\alpha}$ and $\Psi_n{}^{\alpha}$ denote the m-th and n-th excited states of the α-type wave function (a-active), and $\Psi_m{}^{\beta}$ and $\Psi_n{}^{\beta}$ denote those of the β-type wave function (b-active). The intermolecular interaction terms, V_{ij}, have a similar meaning in Eq. 2; they have been evaluated using the direction of the transition moments predicted by Ham and Rudenberg (l, m, n and o for the ^1B_b, ^1B_a, ^1L_a and ^1L_b states respectively). The results of the calculation are shown in Appendix I; the terms V_{ij} have been determined by the use of experimental values of the transition moment. We considered four vibrational sub-levels for the ^1L_a state; the resultant secular equation of the seventh degree is shown in Appendix II. The final result is compared with the observed values in Table II and Fig. 6.

For the first ^1L_b band the calculated small splitting is in accord with the observed value of nearly zero, but the crystalline band as a whole shifts to red about 400 cm^{-1} from the calculated value. The observed intensity is larger than the calculated value by a factor of about 10 for both a- and b-axes.

The second ^1L_a band shows the vibrational structure in crystal, but the band splitting is unusual. The first 0-0 band shows a splitting of 490 cm^{-1} (the a-axis is higher than the b-axis), while the second 0-1 band shows almost no splitting and the third 0-2 band shows a splitting of the reversed sign −100 cm^{-1} (the a-axis is lower than the b-axis). Such results can not be explained by the first-order exciton theory, since the splitting should be proportional to the intensity of each vibrational level. Second-order calculations, including interaction with a higher state, give a better explanation for those splittings since the calculated value is reversed in sign for higher vibrational progressions. However, the magnitude of the calculated value for the 0-0 band is smaller than the observed value (217 cm^{-1} compared with 490 cm^{-1}), while the first-order splitting is 530 cm^{-1}.

Another way of interpreting small splittings for higher vibrational levels might be to consider a strong coupling of the vibronic excited state with the internal vibration of the molecule, and to think that the vibrational relaxation precedes the excitation transfer. However,

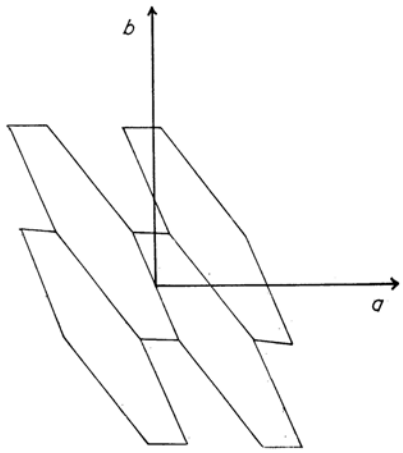

Fig. 5(a) Projection of chrysene molecule onto the (001) plane.

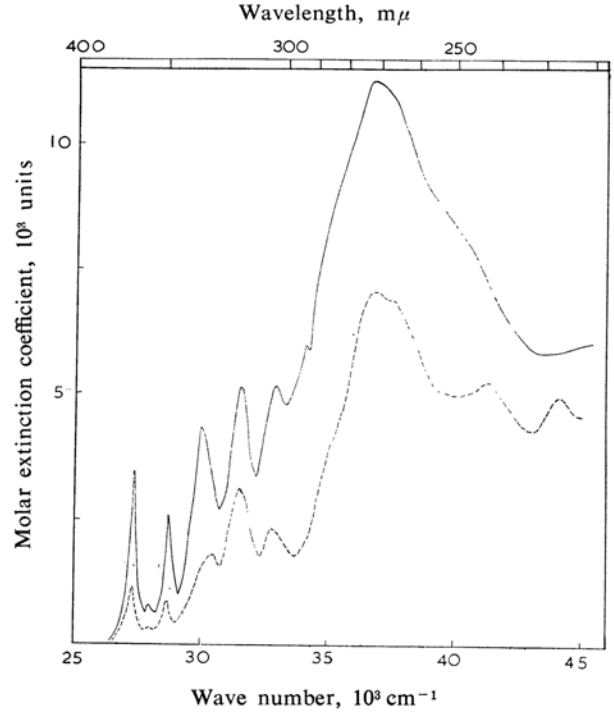

Fig. 5(b) Polarized absorption spectrum of chrysene crystal.

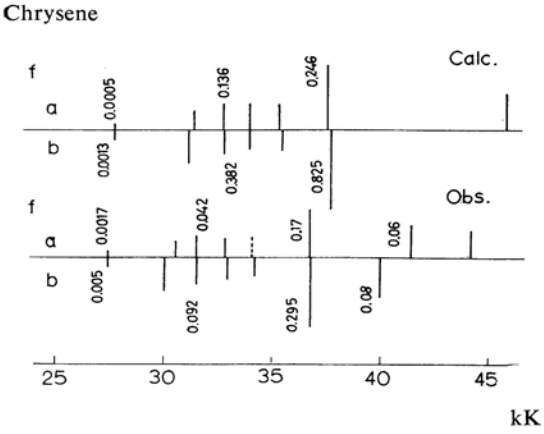

Fig. 6. Calculated and observed band positions of chrysene.

the change in the sign of the splitting can not be explained in this way.

The third ^1B_b band, which is the strongest of all the observed bands in solution, was predicted to be long-axis polarized and should be stronger along the a-axis than along the b-axis. However, both the first- and the second-order calculations show that the ^1B_b band will move to a higher frequency along tha a-axis, and that along the b-axis the ^1B_b and ^1B_a states will appear close together. Therefore, the interpretation of the spectrum in the 37000 cm^{-1} region is that along the a-axis the ^1B_a band appears at a lower frequency than the ^1B_b band, and that the apparent intensity is weakened, since the ^1B_b band moves to a higher frequency. The intensity along the b-axis will be larger than along the a-axis since both ^1B_a and ^1B_b bands are expected to appear in the same region. The second-order calculations demonstrate that the b-axis intensity is stronger than the a-axis in this region and that two bands will be observed along the a-axis while one strong band will appear along b-axis. The observed crystalline spectrum is in fair agreement with this prediction (Fig. 6).

The confirmation of the theory of Ham and Rudenberg[3] concerning the direction of the transition moment is difficult for such an unsymmetrical molecule, because the second-order effect modifies the intensities and positions of each band. However, their theory seems to be correct, since the present calculations, based on their polarization direction, give a satisfactory explanation of the crystalline spectrum.

Azulene

The ultraviolet and visible spectrum of azulene has been measured in a *n*-heptane solution (Fig. 7 (a), (b) and Table III). A theoretical assignment was made by Pariser;[11]

11) R. Pariser, *J. Chem. Phys.*, **25**, 1112 (1956).

his results are also included in Table III. The crystal structure of azulene was determined by Robertson, Shearer, Sim and Watson,[12] who established that the structure is disordered in such a way that successive azulene molecules are subject to a random reversal of direction. Such disorder in the crystal must be taken into account in the calculation of exciton-type interaction. However, it is verified that it is not necessary to change the usual treatment, since the allowed transition will occur when the molecular transition moments are taken in phase for the specified crystal directions. In Fig. 8 this situation is illustrated for the two molecules in an unit cell. The arrows in the figure indicate the direction of the transition moment reversed in the direction of the molecule B from Fig. 8(a) to Fig. 8(b). The allowed combination in Fig. 8 (a) is $\phi_A'\phi_B-\phi_A\phi_B'$ for the a-axis and $\phi_A'\phi_B+\phi_A\phi_B'$ for the b-axis, while in Fig. 8(b) it is $\phi_A'\phi_B+\phi_A\phi_B'$ for the a-axis and $\phi_A'\phi_B-\phi_A\phi_B'$ for the b-axis, where ϕ_A and ϕ_A' indicate the wave function of the A molecule in the ground and the excited states and ϕ_B and ϕ_B' are those for the B molecule. The sign of the dipolar interaction energy is reversed in Fig. 8(b) from Fig. 8(a); it follows that the splitting of the band is not changed by the reversal of the direction of the molecule. This relation can be extended for an infinite number of molecules in the crystal. The second-order calculation of band splitting is performed with a method similar to that described in the previous paragraphs. The calculated dipole-dipole interaction energy is shown in Appendix I, and the secular equation is given in Appendix II. The calculated rerults are compared with the experimental results in Fig. 9 and Table III.

For the first and the second bands, Sidman and McClure[13] had previously measured the polarization in the mixed crystal of azulene in naphthalene. Hunt and Ross[14] published a

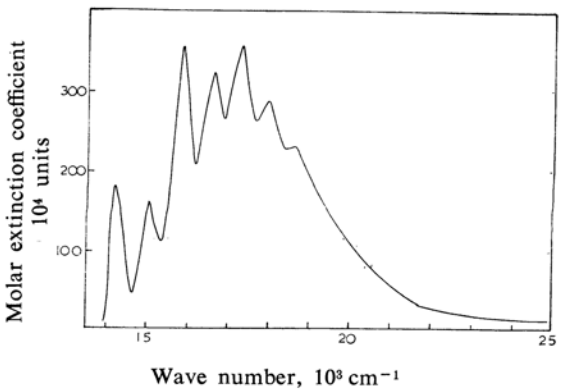

Fig. 7 (a). Visible absorption spectrum of azulene in *n*-heptane.

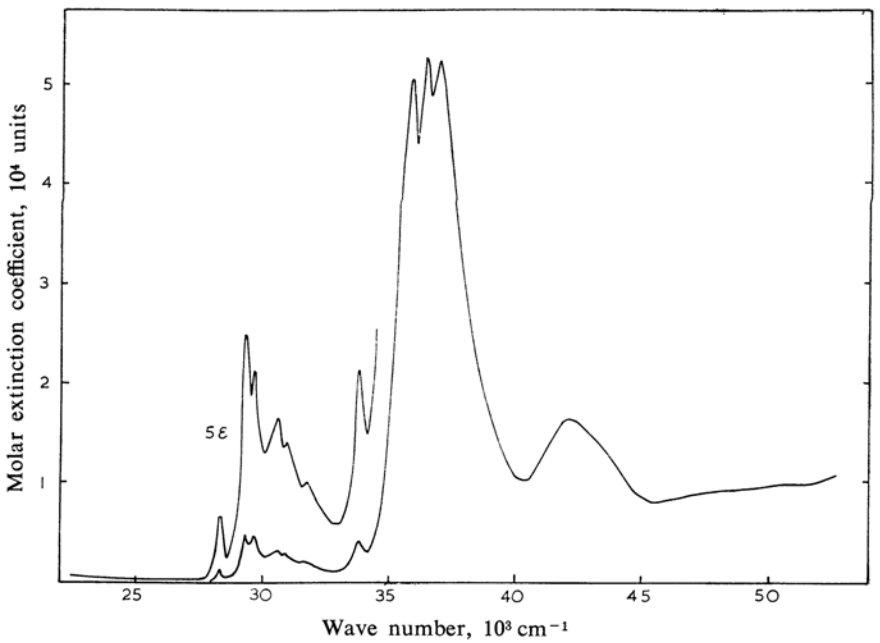

Fig. 7 (b). Ultraviolet absorption spectrum of azulene in *n*-heptane.

12) J. M. Robertson, H. M. M. Shearer, G. A. Sim and D. G. Watson, *Acta Cryst.*, **15**, 1 (1962).

13) J. Sidman and D. S. McClure, *J. Chem. Phys.*, **24** 757 (1955).

14) G. R. Hunt and I. G. Ross, *J. Mol. Spect.*, **9**, 50 (1962).

TABLE III. ABSORPTION BANDS OF AZULENE

	Solution			Crystal (Observed)			Crystal (Calculated)		
	cm^{-1}	f	μ	a-axis	b-axis	$f_a : f_b$ (d. r.)*	a-axis	b-axis	$f_a : f_b$ (d. r.)
	14220			14500	14500				
	15110			15250	15250				
	15850			16000	16000				
^1B	16600	0.0065		16750	16750	0.003 : 0.015			0.004 : 0.015
	17300			17300	17300	(1.0 : 5.0)			(1.0 : 4.8)
	17950			18100	18100				
	18650			19000					
				19600					
	28300								
	29300			27540	27540		29575	28593	0.0025 : 0.0013
^1A	29630	0.048	0.40	29240	29540	0.014 : 0.036			(1.9 : 1.0)
	30650				30230	(1.0 : 2.5)			
	31750								
^1B	33800	0.013	0.18	33530	33470	0.053 : 0.10	33757	32614	0.01 0.02
				34750	34360	(1.0 : 1.8)		33813	0.032
									(1.0 : 5.2)
	35830					0.077	41029		0.260
^1A	36400	0.765	1.40	40700					
	36960								
^1B	42100	0.27	0.77		41400	0.225	43715	41849	0.036 : 0.635
						(1.0 : 3.0)			(1.0 : 2.5)

* The oscillator strength f for the crystal is estimated by using a value of 0.3 μ thickness for the crystal shown in Fig. 8(b).

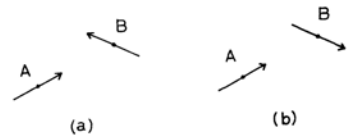

Fig. 8. Direction of transition moment in the azulene crystal.

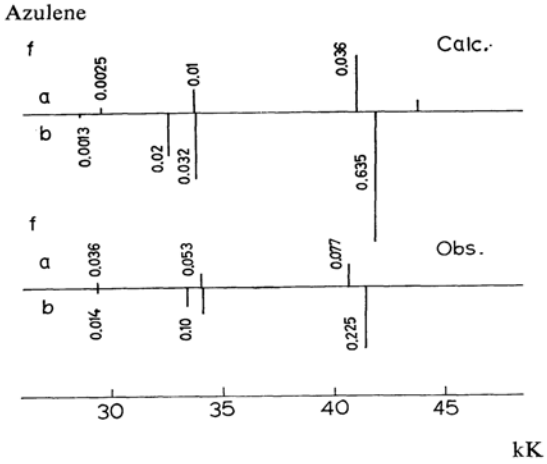

Fig. 9. Calculated and observed band positions of azulene.

pure crystal spectrum for the longer wavelength region; both pairs of authors concluded that the first band is polarized along the short-axis of the molecule. In the present study the pure crystal spectrum has been measured through the (001) plane by a polarized light, as is shown in Fig. 10(b). The projection of molecules according to X-ray results is pictured in Fig. 10(a). The band positions of the visible band are in good agreement with

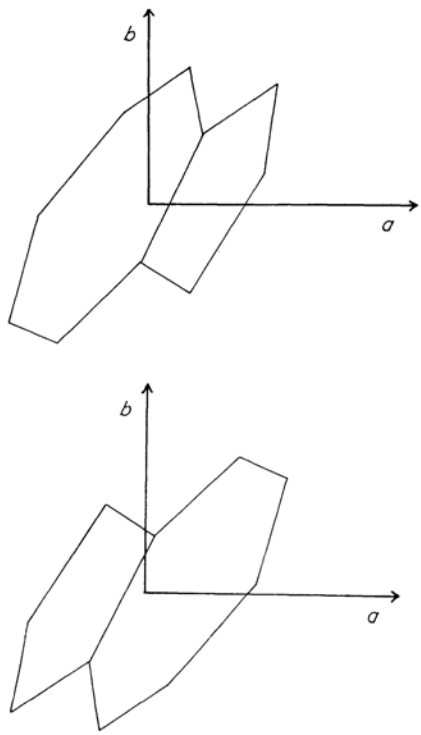

Fig. 10 (a). Projection of the azulene molecule onto the (001) plane.

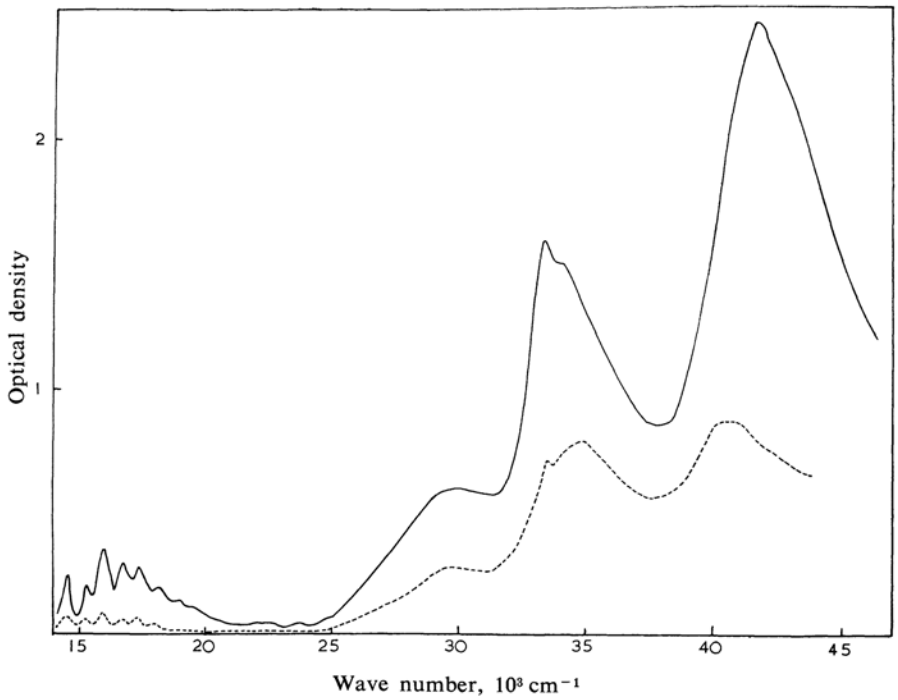

Fig. 10 (b). Polarized absorption spectrum of azulene crystal.

the results of Hunt and Ross within a range of experimental error of $\pm 50\,cm^{-1}$. The dichroic ratio is $D_b : D_a = 5 : 1$; this is in good agreement with the oriented gas value of the short-axis polarization ($D_b : D_a = 4.8 : 1.0$). Since the visible band is situated far from the stronger transitions at higher frequencies, it is possible to treat this band separately from the other transitions. The observed dichroic ratio is in good agreement with the short-axis polarization ratio, so the band may be deduced to be a B-type.

For the second band, Sidman and McClure[13] confirmed the polarization to be long-axis by mixed crystal measurement. Both the present results and the earlier results by Wolf[15] have shown that the absorption is stronger along the b-axis than along the a-axis. If we compare the intensity ratio obtained by the simple oriented gas model with our present results, the dichroic ratio is not in conformity with the long-axis polarization. By the second-order interaction calculation the calculated intensity is still stronger along the a-axis than along the b-axis, but the dichroic ratio is certainly improved. This is mainly due to the interaction with the strongest allowed transition (long-axis polarized), which increases the b-axis intensity and decreases the a-axis intensity. The observed intensity relation might be explained in this way; however, the calculated splitting of $980\,cm^{-1}$ is not clearly observed in the crystal spectrum.

The third band, which has been observed in solution as a shoulder on the tail of a very strong fourth band, is assigned by Pariser to a short-axis polarized B-type band. By a second-order calculation this band is calculated to appear at about $33800\,cm^{-1}$ in both the a- and b-axes, the latter being stronger than the former. In the observed crystal spectrum, the dichroic ratio is in good agreement with these predictions that the b-axis band is stronger than the a-axis and that they will appear at about $33500\,cm^{-1}$.

The fourth absorption band, which is the strongest of all, was shown by Pariser to be a long-axis polarized A-type band. The first order exciton splitting calculation shows that the band should be split very greatly and that the b-axis absorption should be lower in frequency than the a-axis. The second-order calculation shows that it will appear along the b-axis at about $32600\,cm^{-1}$ and along the a-axis at about $41030\,cm^{-1}$. Therefore, the spectrum of the crystal is explained in such a way that the b-axis band is overlapped with the third band and the a-axis band is removed to a higher frequency, at about $40500\,cm^{-1}$.

The fifth band, which was predicted to be of the short-axis polarized B-type, is expected to appear along the b-axis at about $41850\,cm^{-1}$

15) H. C. Wolf, *Solid State Physics*, **9**, 1 (1959).

with the largest intensity and along the a-axis at 43715 cm^{-1} with a smaller intensity. The observed band at 41700 cm^{-1} along the b-axis is assigned to this origin, but along the a-axis the band is not clearly seen because the shifted fourth band overlaps it in this region.

In this way, all the crystalline absorption bands are correlated with the calculated energy levels, but the changes from molecular levels to crystalline states are so complicated that it is difficult to give an explanation of the nature of the crystalline transition by a one-to-one correspondence with each molecular absorption band. The second-order calculation based on Pariser's assignment is shown to be satisfactory in explaining the whole pattern of the crystalline spectrum, but still there remain some discrepancies between the observed and the calculated splittings and intensities. The calculated intensities show a big difference between the

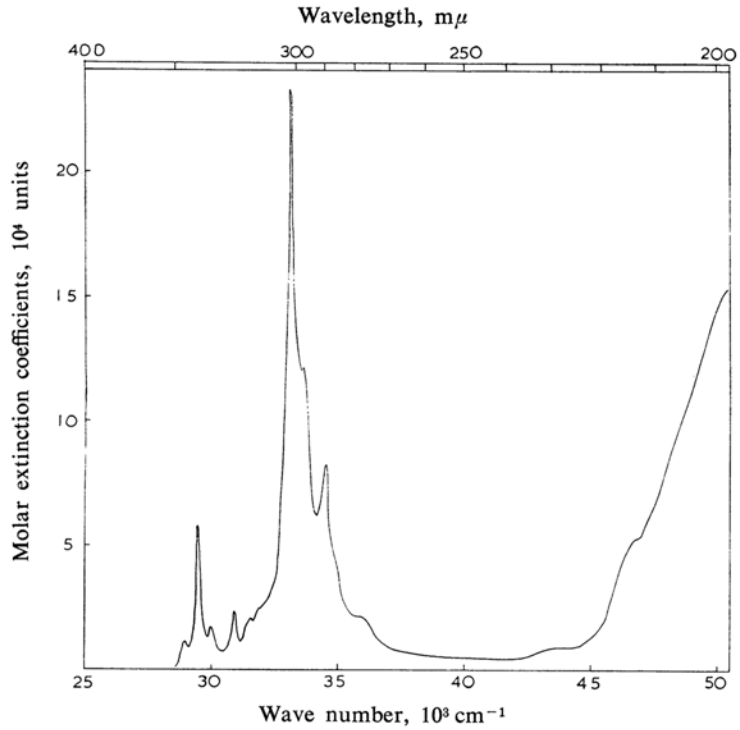

Fig. 11. Absorption spectrum of coronene in ethanol.

TABLE IV. ABSORPTION BANDS OF CORONENE

	Solution			Crystal (Observed)				Crystal (Calculated)			
	cm^{-1}	f	μ	a-axis	b-axis	splitting	$f_a : f_b$ (d. r.)	a-axis	b-axis	splitting	$f_a : f_b$ (d. r.)
$^1B_{2u}$				22130 23250 24140 24600	22130 23250 24190 24640						
$^1B_{1u}$	29000 29490 30000 30930 31600 31950	0.100 0.090	0.56	27150 28250 29950	27250 28450 30230 31850	200	0.08 : 0.03 (2.7 : 1.0)	29058	29497	439	0.39 : 0.03 (13 : 1)
$^1E_{1u}$	33200 33700 34600 35850 43900 46500	1.34	0.76 0.76	31410 33570 36440	34560	3200	0.33 : 0.23 (1.4 : 1.0)	30359 39335	33129 36084	2770	1.06 : 0.87 (1.2 : 1.0) 0.002 : 0.01

* The oscillator strength of crystal is tentatively determined by assuming the value of birefringence of 0.1 between the b- and a-axes.

strong and weak bands, but the observed spectrum shows a rather stronger mixing, so that there must be unknown mechanism which changes the intensity of the crystalline band.

Coronene

The ultraviolet absorption spectrum of coronene has been measured in an ethanol solution; three strong absorption bands were observed, as Fig. 11 and Table IV show. In a benzene solution another weaker band is observed in the region of 23400 cm^{-1}. The crystal spectrum has been recorded through the (001) plane; it is shown in Fig. 12(b). The crystal structure was determined by Robertson and White,[16] and the projection of molecules onto the (001) plane is pictured in Fig. 12(a). The characteristics of the spectrum resemble these of benzene since coronene has a symmetry like that of D_{6h}. The first weak band at 23400 cm^{-1} may correspond to the 2600 Å band of benzene ($^1B_{2u}$); the band in the 29000 cm^{-1} region, to the 2000 Å band of benzene ($^1B_{1u}$), and the strongest band at 33000 cm^{-1}, to the 1800 Å band ($^1E_{1u}$).

In the free coronene molecule the transition to the $^1B_{1u}$ state is possible along the three two-fold symmetry axes passing through carbon atoms (three axes like m in Fig. 13), and the transition to the $^1B_{2u}$ state is possible along the other three two-fold axes (three axes like l in Fig. 13). Davydov[1] has discussed the relation between the symmetry of the molecular excited state and that of the crystalline state, but his argument may be justified only when the molecular symmetry axis coincides with the crystalline symmetry axis. In crystal coronene one of the m-axis (with the direction cosines of $m_a=0.7174$, $m_b=0.6865$ and $m_{c'}=-0.1188$) is nearly perpendicular to the c'-axis. Therefore, we will assume that this axis is the pseudo-two-fold unique symmetry axis of coronene in crystal. Namely, the crystal symmetry operation, C_2^b, may correspond to the transposition of the molecule

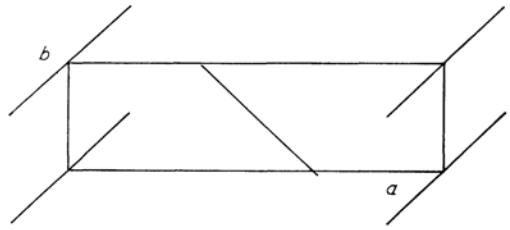

Fig. 12 (a). Projection of coronene molecule onto the (001) plane.

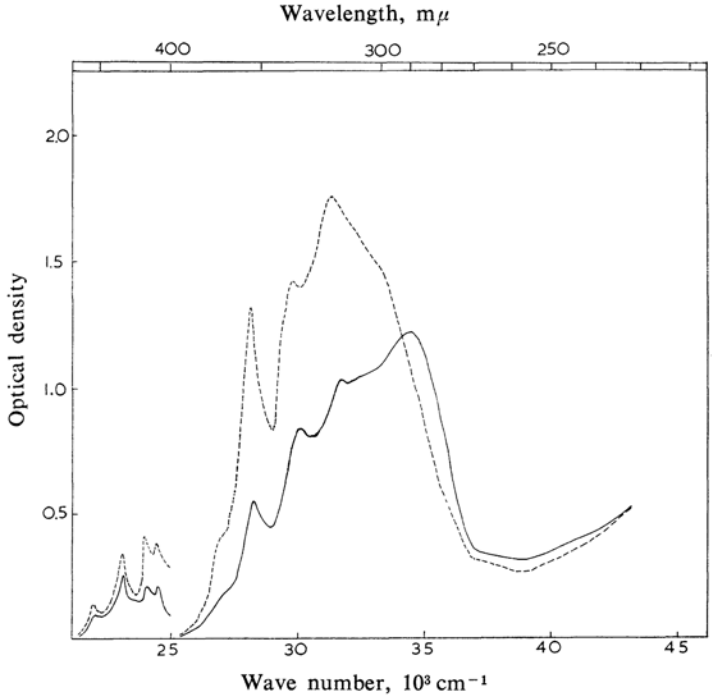

Fig. 12 (b). Polarized absorption spectrum of coronene crystal. (The retardation in the thin crystal (right curve) is about 25 mμ and that in the thick crystal (left curve) is 190 mμ.)

16) J. M. Robertson and J. G. White, *J. Chem. Soc.*, **1945**, 607.

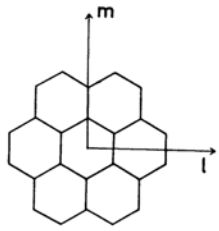

Fig. 13. Coronene.

at the origin to the (1/2, 1/2, 0) position, followed by a rotation of 180° around the m-axis and a rotation of about 90° around the l-axis. In this situation the degeneracy of the electronic transitions might be removed so that the m-axis may be taken as an axis along which the transition to the $^1B_{1u}$ state is possible. From the intensity relations observed in the crystal spectrum, it seems certainly correct to choose the m-axis as an unique two-fold symmetry axis, since the 29000 cm^{-1} band is observed strongly in crystal, while the 22000 cm^{-1} band is very weak. The 22000 cm^{-1} band is supposed to be strengthened in intensity in crystal by mixing with stronger transitions, but in reality the band is observed very weakly in crystal; therefore, the direction of the transition moment is considered to be on the l-axis, which is nearly vertical to the (001) plane.

Lyons and Walsh[17] have calculated the first-order splitting of the $^1E_{1u}$ level, but they did not pay any particular attention to the interaction with the $^1B_{1u}$ state. Actually the observed band shows a mixing of the $^1B_{1u}$ state with the $^1E_{1u}$ state; namely, the intensity of the absorption band at 29000 cm^{-1} is far less than that of the 33000 cm^{-1} band in solution, while it becomes comparable in crystal. Therefore, it might be necessary to include the interaction between the $^1B_{1u}$ state and two $^1E_{1u}$ states. The first-order wave function for each excited states may be given by the following formulae:

$$\left.\begin{aligned}\Psi^{\alpha} &= \frac{1}{\sqrt{2N}}\left(\sum_{i=1}^{N}\phi_{1i}' - \sum_{j=1}^{N}\phi_{2j}'\right)\\ \Psi^{\beta} &= \frac{1}{\sqrt{2N}}\left(\sum_{i=1}^{N}\phi_{1i}' + \sum_{j=1}^{N}\phi_{2j}'\right)\end{aligned}\right\} \quad (9)$$

where Ψ^{α} and Ψ^{β} represent the wave functions which are active along the a- and b-axes respectively. The functions ϕ_{1i}' and ϕ_{2j}' indicate that a molecule at the $1i$-th or $2j$-th site is excited and that the others are in their ground state. The dipole-dipole interaction energies have been calculated over molecules within 20 Å and 40 Å radius spheres; they are shown in Appendix I. The figures for the 40 Å radius summation are in excellent agreement with the values of Lyons and Walsh who employed the Ewald-Kornfeld method for infinite summation, so that the convergence of the summation seems to be sufficient by 40 Å for such a large molecule.

The assignment of the crystalline absorption bands is very much complicated by the presence of the vibrational structures. We have tentatively decided on the assignments shown in Table IV, taking the 31300 cm^{-1} band along the a-axis and the 34500 cm^{-1} band along the b-axis as the split $^1E_{1u}$ components. The other peaks around 28000—32000 cm^{-1} are ascribed to the vibrational progressions of the $^1B_{1u}$ band. The first-order band splitting of the $^1E_{1u}$ level, considering the degeneracy of the band, is 3110 cm^{-1}, while the observed value will be 3200 cm^{-1} if we follow the assignment mentioned above. The value suggested by Lyons and Walsh was 3615 cm^{-1}; their value might be larger than ours because they used a larger transition dipole moment.

As has been mentioned previously, a characteristic feature of the crystalline spectrum is the mixing of the $^1B_{1u}$ state with the $^1E_{1u}$ state; therefore, the second-order calculations have been made with the first $^1B_{1u}$ state and two degenerate $^1E_{1u}$ levels. The higher $^1B_{1u}$ progressions are disregarded since they are situated close to the $^1E_{1u}$ state. The first trial using the solution's intensity data gave too strong a coupling between the $^1B_{1u}$ and $^1E_{1u}$ states, so we have reduced the magnitude of the transition dipole for the $^1B_{1u}$ state to half of the observed value. The calculated results are compared with the experimental results in Fig. 14 and Tabe IV. It is found that the general pattern of the spectrum is

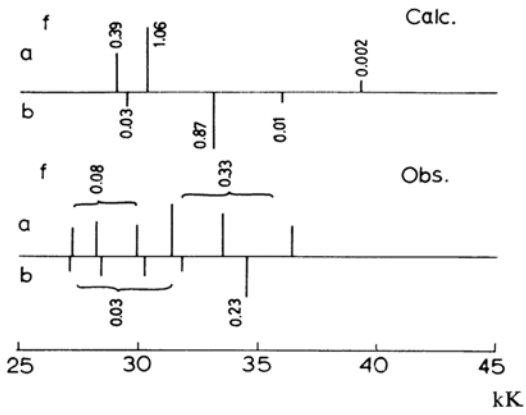

Fig. 14. Calculated and observed band positions of coronene.

17) L. E. Lyons and J. R. Walsh, ibid., 1959, 3447.

rather well reproduced in the calculations, particularly in intensity relations between the $^1B_{1u}$ and $^1E_{1u}$ states, but the splittings are slightly smaller than the observed values. Presumably a more complicated interaction will occur between the $^1B_{1u}$ and $^1E_{1u}$ states in crystal by the electron exchange or another effect, because the electron overlap along the b-axis is expected to be large.

The use of a smaller transition moment for the $^1B_{1u}$ state is possible if we think that the band is originally forbidden in character but appears through the vibrational coupling.

The absorption tail at about 38000 cm^{-1}, which continues to the shorter ultraviolet region, may involve a transition to the Rydberg series or to the continuous band.

Tetracene

The electronic absorption spectrum of tetracence in ethanol and in a crystal has been measured as is shown in Figs. 15 and 16(b). Pariser[18] calculated the energy levels of the molecule; the bands at 21000 cm^{-1} and 34000 cm^{-1} were shown to be short-axis (M-axis) polarized, while the 36400 cm^{-1} band is long-axis (L-axis) polarized. Another transition at about 60000 cm^{-1} was also predicted to be an M-axis polarized band.

The crystal spectrum was measured by Bree and Lyons,[19] but they did not discuss the results with reference to the crystal structure. The present results are nearly in agreement with theirs; in addition, the shape of the 46000 cm^{-1} band is confirmed to be at a shorter

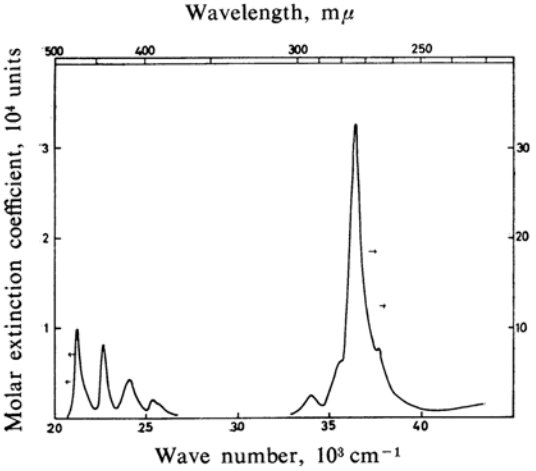

Fig. 15. Absorption spectrum of tetracene in ethanol.

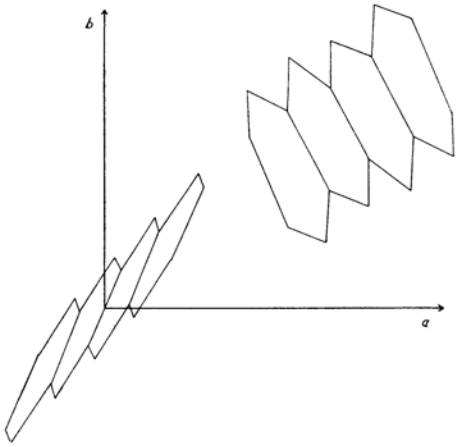

Fig. 16(a). Projection of tetracene molecules onto the (001) plane.

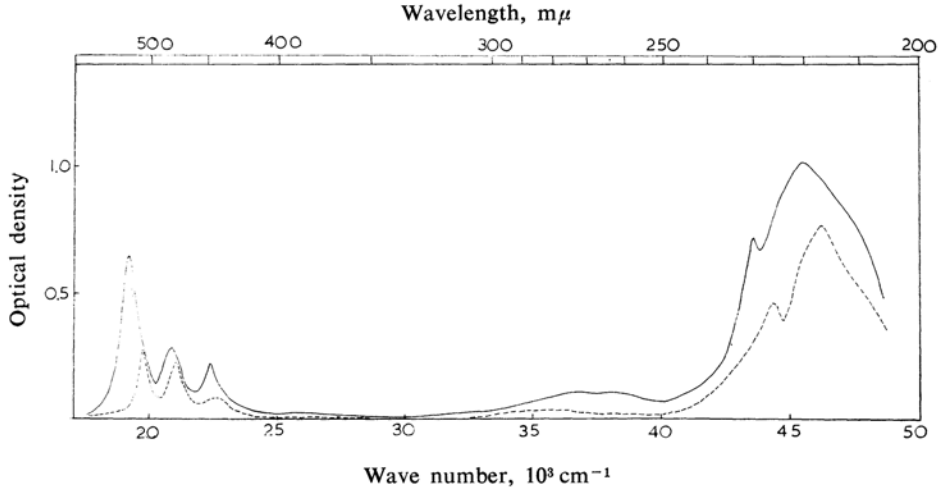

Fig. 16 (b). Polarized absorption spectrum of tetracene crystal.

18) R. Pariser, *J. Chem. Phys.*, **24**, 250 (1956).

19) A. Bree and L. E. Lyons, *J. Chem. Soc.*, **1960**, 5206.

TABLE V. ABSORPTION BANDS OF TETRACENE

	Solution			Crystal (Observed)				Crystal (Calculated I)			Crystal (Calculated II)			
	cm^{-1}	f	μ	a-axis	b-axis	split	$f_a : f_b$	a-axis	b-axis	split.	a-axis	b-axis	split.	$f_a : f_b$
$^1B_{2u}$	21200	0.025	0.33	19861	19231	630	0.007 : 0.027	21062	21032	30	21062	21045	17	0.012 : 0.058
	22620	0.020	0.29	21186	20964	222	0.006 : 0.014	22527	22509	18	22528	22516	12	0.009 : 0.047
	24100	0.017	0.26	22760	22607	153	0.004 : 0.006 (1.0 : 2.8)	24030	24016	14	24030	24021	9	0.008 : 0.040 (1.0 : 5.1)
$^1B_{2u}$	34000	0.086	0.48	35670	34000			33747	30736		33764	33369		
					36400				33650			33665		
$^1B_{3u}$	35600	1.3	1.81	44340	43480	860	0.15 : 0.24	50555	50555	0	43526	43526	0	0.25 : 0.25
	36400			46080	45455	625	(1.0 : 1.6)							(1.0 : 1.0)
	37650													

ultraviolet region. The crystal structure has been determined recently by Robertson, Sinclair and Trotter;[20] they have found that the crystal is triclinic with the space group of $P\bar{1}$ (cf. Fig. 16(a)). For this crystal symmetry the selection rule which is strict for the crystal of a higher symmetry does not hold, and possible transitions are observed in all directions of the crystal. The excited state wave functions are:

$$\Psi^{\alpha}=\frac{1}{\sqrt{2N}}\left(\sum_{i=1}^{N}\phi_{1i}'+\sum_{j=1}^{N}\phi_{2j}'\right)$$

$$\Psi^{\beta}=\frac{1}{\sqrt{2N}}\left(\sum_{i=1}^{N}\phi_{1i}'-\sum_{j=1}^{N}\phi_{2j}'\right)$$

where ϕ_{1i}' represents the state in which the molecule on the $1i$-th site is excited and the others are in their ground state. These two types of excited-state wave functions will behave differently in intensity relations. Following the crystal structure data, it is found that the M-axis polarized band is stronger for the Ψ^{α} state along the b-axis than along the a-axis, while for the Ψ^{β} state the situation is reversed. The L-axis polarized band will appear only for the Ψ^{α} state in both a- and b-axes directions, and the band for the Ψ^{β} state will be very weak. The dipole interaction energies have been calculated for every combination of directions of the transition moment on 1st-site and 2nd-site molecules, as Appendix I shows.

The band observed near $20000\,cm^{-1}$ is assigned to the M-axis polarized band on the basis of the dichroic intensity ratio. The b-axis polarized band is considered to be the transition to the Ψ^{α} state, while the a-axis band is regarded as arising from the Ψ^{β} state. The first-order dichroic ratio is;

$$D_b : D_a=(\cos m_b(\mathrm{I})+\cos m_b(\mathrm{II}))^2/(\cos m_b(\mathrm{I})-\cos m_b(\mathrm{II}))^2$$
$$=5.1 : 1.0$$

where $m_b(\mathrm{I})$ indicates the angle between the b-axis and the M-axis of the 1st site molecule. The observed dichroic ratio is 2.8 : 1.0. The results of the calculation of splitting between the Ψ^{α} and Ψ^{β} states are shown in Table V, where it is shown that the calculated value is less than $30\,cm^{-1}$ according to a weak coupling model. The observed value is as large as $630\,cm^{-1}$; even when a strong coupling model is employed, the calculated value does not exceed $130\,cm^{-1}$. Presumably the interaction involving electron exchange and the charge transfer effect might be important in explaining this splitting. Near the $37000\,cm^{-1}$ region in the crystal another band is observed which is regarded as the M-axis polarized band observed in solution at $34000\,cm^{-1}$.

The strongest L-axis polarized band, situated at $36000\,cm^{-1}$ in solution, is expected to split into Ψ^{α} and Ψ^{β} states in the crystal. The first-order band shift is calculated to be about $14000\,cm^{-1}$ for the Ψ^{α} stated and $-6000\,cm^{-1}$ for the Ψ^{β} state. Actually, the Ψ^{α} state is shifted about $8000\,cm^{-1}$ to a higher frequency and the Ψ^{β} state, although it can not be clearly seen, seems to be unchanged in position and to overlap with the M-axis polarized band. The Ψ^{β} state is calculated to appear more strongly along the b-axis than along the a-axis, so that the extra band along the b-axis near $34000\,cm^{-1}$ might be explained by this origin. The observed smaller shift of the Ψ^{α} state can be explained if we use a smaller value of the transition dipole in crystal; the second-order calculation value using $1/\sqrt{2}$ of the solution's f-value is shown in Table V. The Ψ^{α} state shows a splitting of $800\,cm^{-1}$ between the b- and a-axes; such a result cannot be explained by the present calculations. A possible mechanism for this shift is interaction with the higher ionized state in the crystal.

With regard to the band position of the first $^1B_{2u}$ band, the present results are in good agreement with the earlier results of Bree and Lyons, but the present intensity is not in

20) J. M. Robertson, V. C. Sinclair and J. Trotter, *Acta Cryst.*, **14**, 697 (1961).

accordance with theirs. The prsent measuerement of the thickness of the crystal is not as accurate because we have determined the thickness by a retardation of the crystal as measured by a compensator, which might be in error by as much as 20%. The molar extinction coefficient of the first peak is estimated to be $\varepsilon_b = 6300$; this is a half of the value of Bree and Lyons. However, our oscillator strength is larger than theirs, since we have used the usual formula for the oscillator strength instead of that for the reduced oscillator strength. The theoretical intensities are compared with the experimental values in Table V; it is remarkable that the second calculation using the smaller transition dipole for the $^1B_{3u}$ state gives nearly the correct size of the oscillator strength in the crystal. The intensity of the first $^1B_{2u}$ state is smaller than the calculated value; therefore, it seems certain that a general hypochromism occurs in the crystal of tetracene.

Discussion

When the observed band splittings and intensities are compared with the calculated values, the second-order theory, which includes interactions between several excited levels, is shown to be better than the first-order calculation. In crystals such as azulene and chrysene, the first-order intensity relations are so greatly changed that the direction of the transition moment can not be simply determined from the dichroic intensity ratio for each band. This is quite contrary to the case of substituted benzenes,[2] where the direction of the transition moment has been nicely determined from the intensity relations. When these two cases are examined in the off-diagonal (H_{ij}) and the diagonal matrix element (H_{ii}, H_{jj}) in the second-order secular equation, it is found that a big deviation occurs when the term

$$H_{ij}/H_{ii}-H_{jj}$$

becomes large enough to make for an efficient mixing of several excited states. In cases of substituted benzenes, the separation of each band, $H_{ii}-H_{jj}$, is relatively large, and the off-diagonal term is smaller because of the small magnitude of the transition moment; hence, the simple oriented gas model holds rather well. In the aromatic hydrocarbons described in the present paper, an efficient mixing of excited levels occurs under favorable conditions of large interaction terms and a narrow spacing of excited states. In this way the larger deviation of the intensity relation from the simple oriented gas rule in azulene and chrysene crystals can be explained.

However, there still remains some question unexplained by the dipolar interaction theory. Namely, in coronene and tetracene crystals the calculated splittings do not agree with the observed values. One possible reason for these difficulties might be our ignorance of electron overlap and charge transfer effects, which are certainly important in such crystals as pyrene and perylene.[7] The matrix element, including the electron overlap effect, has been disregarded in the present calculations; however, it would be significant if we consider the interaction between the exciton state and the charge transfer state.[8] Because of the small ionization potential and the large electron affinity of aromatic hydrocarbon molecules, the diagonal element of the charge-transfer state would be comparable in energy to some exciton state, and the off-diagonal term includes the energy which is first-order with the electron overlap. In recent notes[21] some authors have stressed the importance of electron exchange effect in triplet exciton, the magnitude of which has been estimated to be about 5 to 10 cm^{-1}, but the effect might be second-order to the electron overlap, which should be one to two orders of magnitude smaller than the present consideration of interaction energy. Therefore, the charge-transfer electron overlap effect may be important in the calculation of splitting, since its magnitude may reasonably be guessed to amount to several hundred reciprocal centimeters under favorable conditions. This point will be explored in a further study.

Summary

The electronic absorption spectra of single crystals of pyrene, chrysene, azulene, coronene and tetracene have been measured by a polarized light. Some crystal absorption bands exhibit appreciable splittings and changes in intensity relations according to the simple exciton theory. Those results are explained by the use of the second-order exciton calculation without the inclusion of the electron overlap effect. The theoretical results give a fairly reasonable explanation of crystal spectra, and it has been shown that the second-order mixing of excited states plays an essential role in modifying the crystal spectra from the pattern of the free molecule.

The author would like to thank Professor Saburo Nagakura for his encouragement throughout this work. He would also like to express his gratitude to Professors Hideo Akamatu and Hiroo Inokuchi for their gifts

21) G. C. Nieman and G. W. Robinson, *J. Chem. Phys.*, 37, 2150 (1962); J. Jortner, S. Choi, J. L. Katz and S. A. Rice, *Phys. Rev. Let.*, 11, 323 (1963).

of samples, and to Professor David P. Craig for his kind communication on dipole interaction energies.

The Institute for Solid State Physics
The University of Tokyo
Azabu, Tokyo

Appendix I

Dipole Interaction Energies ($cm^{-1}/Å^2$)

*Pyrene**

	l-l	m-m	n-n	l-m	l-n	m-n	N. S.
1-1	−19	−59	81	371	−338	−185	510
	(−26)	(−58)	(88)	(373)	(−332)	(−171)	108
1-2	−769	−1731	2494	54	−2043	126	504
	(−767)	(−1741)	(2501)	(40)	(−2046)	(120)	106
1-3	−676	−281	−324	201	−151	−344	504
	(−669)	(−292)	(−334)	(197)	(−152)	(−340)	108
1-4	38	−324	−629	−664	392	78	504
	(32)	(−348)	(−650)	(−659)	(384)	(76)	112

*Azulene**

	l-l	m-m	n-n	l-m	l-n	m-n	
1-1	648	−813	172	−48	146	735	1462
	(658)	(−830)	177	(−68)	(139)	(751)	304
1-2	−2715	250	1976	855	1130	1074	1432
	(−2759)	(236)	(1987)	(859)	(1134)	(1092)	316

*Coronene***

	l-l	m-m	n-n	l-m	l-n	m-n	
1-1	1994	−839	−1157	−41	−671	−3678	376
	(2091)	(−883)	(−1211)	(−100)	(−629)	(−3671)	42
1-2	−497	903	957	440	−293	−257	372
	(−536)	(868)	(912)	(405)	(−262)	(−276)	48

*Tetracene**

	l-l	m-m	l-m
1-2	1175	−981	907
	(1156)	(−973)	(864)
2-2	1235	−1274	497
	(1214)	(−1250)	(485)
1-2	3030	22	81
	(2998)	(34)	(80)
2-1	3030	22	1615
	(2998)	(34)	(1619)

*Chrysene****

	l-l	m-m	n-n	o-o	l-m	l-n	m-n	l-o	m-o	n-o
1-1	1877	−1483	792	−260	−378	1748	782	671	−1378	1529
1-2	−719	408	−420	405	165	−688	−173	−269	364	−479
1-3	−3523	78	−2913	−1000	709	−3307	456	−1492	−4	−1192
1-4	724	216	657	352	−87	635	−220	337	186	130

The directions of the transition dipoles are referred to the long (l), short (m) and normal (n) axes of the molecule for pyrene, azulene, coronene and teracene. The directions for chrysene are shown below. N. S. means the number of molecules summed.

* Numbers without bracket are for 50Å-radius summation and those in bracket are for 30Å-radius summation.

** Numbers without brackets are for 40Å-radius summation and those in brackets are 20Å-radius summation.

*** The summation was taken for a 30Å-radius sphere only.

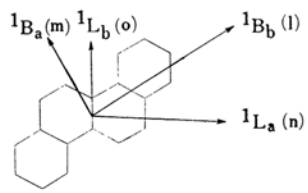

Appendix II

Matrix Elements for the Secular Equations of the Excited States

Pyrene

α

^1L_b	26884					
^1L_a(I)	−4	30236				
^1L_a(II)	−4	274	31739			
^1L_a(III)	−3	181	157	32954		
^1B_a	54	−56	−49	−32	37396	
^1B_b	−9	632	550	362	−113	42748

β

^1L_b	26926					
^1L_a(I)	39	29941				
^1L_a(II)	34	18	31516			
^1L_a(III)	22	12	11	32857		
^1B_a	57	494	428	283	37433	
^1B_b	78	42	37	24	989	41565

Chrysene

α

^1L_b	27730						
^1L_a	49	31760					
	44	369	33082				
	40	335	301	34304			
	35	293	266	240	35628		
^1B_b	−4	2120	1910	1730	1520	44610	
^1B_a	60	283	254	231	202	−960	37434

β

^1L_b	27730						
^1L_a	20	31219					
	18	−118	32644				
	17	−107	−96	33943			
	15	−94	−84	−71	35486		
^1B_b	97	57	47	43	38	37615	
^1B_a	70	398	358	325	285	24	37728

Azulene

α

A	29840			
B	−65	33766		
A	1880	−228	43000	
B	−278	−147	−975	41470

β

A	28970			
B	58	33782		
A	−1152	204	32350	
B	248	−78	870	41767

Coronene

α

$^1B_{1u}$	29400		
$^1E_{1u}$(m)	−560	30100	
$^1E_{1u}$(l)	−155	−866	39253

β

$^1B_{1u}$	29500		
$^1E_{1u}$(m)	20	33315	
$^1E_{1u}$(l)	128	718	35895

Tetracene

α

$^1B_{2u}$	21078				
	−110	22526			
	−99	−87	24024		
$^1B_{2u}$	−182	−160	−144	33736	
$^1B_{3u}$	−87	−77	−69	−127	30378

β

$^1B_{2u}$	21083				
	−106	22529			
	−95	−83	24027		
$^1B_{2u}$	−175	−154	−138	33746	
$^1B_{3u}$	925	814	730	1350	50376